Long-Range Order and Orientation of Cylinder-Forming Block Copolymers on Chemically Nanopatterned Striped Surfaces

Erik W. Edwards, Mark P. Stoykovich, Harun H. Solak,† and Paul F. Nealey*

Department of Chemical and Biological Engineering and Center for Nanotechnology, University of Wisconsin−Madison, Madison, Wisconsin 53706, and Laboratory for Micro- and Nanotechnology, Paul Scherrer Institut, Villigen/PSI, Switzerland CH-5232

Received November 1, 2005; Revised Manuscript Received February 28, 2006

ABSTRACT: Cylinder-forming poly(styrene-*b*-methyl methacrylate) (PS-*b*-PMMA) thin films were directed to assemble on chemically nanopatterned surfaces consisting of alternating stripes that were preferentially wet by the two blocks of the copolymer. The cylindrical domains oriented in the plane of the film and formed defect-free periodic arrays over large areas in registration with the underlying chemical surface pattern if three constraints were satisfied: the substrate pattern period (L_S) was commensurate with the bulk intercylinder period of the block copolymer (L_O), the initial film thickness was quantized with respect to the thickness of a half layer ($L/2$) or single layer of cylinders (L), and the widths of adjacent stripes of the chemical surface pattern were nearly equal.

Introduction

Diblock copolymers are polymer molecules consisting of two chemically distinct chains covalently bonded at a single point. When diblock copolymers are annealed above the glass transition temperatures of their constituent components and below an order−disorder transition temperature, they tend to microphase separate to form equilibrium structures including spheres, cylinders, or lamellae with bulk repeat spacings on the order of 10−100 nm.[1,2] The overall molecular weight of the block copolymer, the volume fraction of the two components, and the Flory−Huggins interaction parameter, χ, determine the morphology of the block copolymer and the bulk repeat spacing of the domains. In thin films, diblock copolymers can be used for nanopatterning applications by applying additive or subtractive processes to the block copolymer domain structure to create dense arrays of uniform nanostructures in a process known as block copolymer lithography.[3]

Block copolymer lithography has been developed for cylinder-forming diblock copolymers in thin films with the cylindrical domains oriented either perpendicular or parallel to the substrate. For example, templates consisting of uniform, isolated pores created from the removal of the minority block of cylinder-forming block copolymers have been used in subtractive processes to fabricate increased capacitance gate devices,[4] nanocrystal floating gate devices for FLASH memory,[5] and high-capacity metal oxide semiconductor capacitors.[6] Additive processes have been used on similar templates generated from cylinder-forming diblock copolymers to produce magnetic nanowires,[7] magnetic nanodots,[8] and metallic nanodots[9] that are oriented perpendicular to the substrate. Examples of applications in which cylinder-forming diblock copolymers oriented parallel to the substrate have been used include the fabrication of metallic nanowires[10] and the generation of one-dimensional arrays of spheres through a hierarchical process involving thermally induced phase transitions.[11] An additional advantage of block copolymer lithography rests in the possibility of using the self-assembled domain structures as chemical templates for creating composite materials. Examples of such materials include metal/block copolymer composites that incorporate nanoparticles, nanoclusters, or metallic domains deposited by electroless deposition in or on top of one of the self-assembled block copolymer domains[12−19] and organic/inorganic hybrid materials that selectively incorporate silicon containing moieties in one of the block copolymer domains.[20−23]

In addition to those applications that benefit from the generation of dense arrays of nanostructures with uniform dimensions and spacings, there are many applications that will require block copolymer domain arrays with a high degree of translational and orientational order. Techniques that have been used to create highly ordered arrays of either parallel or perpendicular cylinders include electric field alignment,[24−26] nano-imprint lithography,[27] and topographically patterned substrates or graphoepitaxy.[8,28,29] Additionally, highly ordered perpendicular arrays of cylinders have been fabricated by using solvent annealing,[30,31] and highly ordered parallel arrays of cylinders have been fabricated by using shear alignment.[32]

Previously, we have directed the assembly of lamellae-forming block copolymers on chemically nanopatterned striped substrates to fabricate defect-free arrays of perpendicular domains that are registered with the underlying chemical surface pattern.[33] This technique has been shown to be capable of fabricating both periodic[34] and nonregular device-oriented arrays[35] of block copolymer domains. Here, we demonstrate that thin films of cylinder-forming diblock copolymers can be directed to assemble into defect-free arrays oriented parallel to the substrate when they are annealed on chemically nanopatterned striped surfaces. When the stripes are patterned with periods that are commensurate or near commensurate with the bulk block copolymer intercylinder repeat period, L_O, the periodic preferential wetting of the two blocks of the block copolymer directs the assembly of the cylindrical domains into arrays that are parallel to the substrate and defect-free over large areas.

Experimental Section

Unless otherwise noted, all chemicals were used as received. PS-*b*-PMMA (M_N = 46-*b*-21 kg/mol, PDI = 1.09, L_O = 44.8 nm) was purchased from Polymer Source Inc. of Dorval, Quebec.

* Corresponding author. E-mail: nealey@engr.wisc.edu.
† Laboratory for Micro- and Nanotechnology, Paul Scherrer Institut.

10.1021/ma052335c CCC: $33.50
Published on Web 04/13/2006

Styrene, toluene, and chlorobenzene were purchased from Aldrich Chemical Co. of Milwaukee, WI. Sulfuric acid, hydrogen peroxide, isopropyl alcohol, and methyl isobutyl ketone were purchased from Fisher Scientific. Photoresist-grade poly(methyl methacrylate) (M_N = 950 kg/mol, 6 wt % in chlorobenzene) was purchased from Microchem Corp. of Newton, MA, and diluted to 1.2 wt % in chlorobenzene. Silicon wafers were purchased from MONTCO Silicon Technologies Inc.

Hydroxyterminated polystyrene was synthesized by using a TEMPO-based 2,2,6,6-tetramethylpiperidin-1yl oxide initiator as reported in the literature.[25,34,36−38] Prior to polymerization, styrene monomer was degassed. Polymerization was performed for 3 days under argon at 125 °C. The resulting polymers were dissolved in toluene and precipitated in methanol before drying overnight under vacuum (approximately 30 mTorr).

A 40-nm-thick layer of hydroxyterminated polystyrene was spin-coated onto silicon wafers that were cleaned with piranha solution ((7:3) v/v H_2O_2/H_2SO_4 at 100 °C, for 30 min). (Caution: piranha reacts violently with organic compounds and should not be stored in closed containers.) The silicon wafers coated with hydroxyterminated polystyrene were then annealed under vacuum for 48 h at 160 °C to graft a 4-nm-thick layer of polystyrene, henceforth referred to as a brush, to the silicon substrate. The excess, ungrafted hydroxyterminated polystyrene was then removed by repeated sonication in warm toluene. The resulting polystyrene brush had water contact angles of 93° (advancing) and 79° (receding).

The silicon substrates with polystyrene brushes were spin-coated with a thin layer of poly(methyl methacrylate) photoresist (50 nm) and baked in air at 130 °C for 120 s. The photoresist was then patterned by using extreme ultraviolet lithography (EUVL) as described previously in the literature.[39] The mask used in these experiments yielded topographic patterns in the photoresist consisting of lines and spaces with periods, L_S, ranging from 40 to 50 nm in increments of 2.5 nm. EUV exposures were performed in a vacuum at 10^{-5} mbar at the X-ray interference lithography beamline of the Swiss Light Source. The beamline uses undulator light with a central wavelength of 13.4 nm, 92 eV, and 4% spectral bandwidth.

After exposure, the films were developed in a 1:3 development mixture of methyl isobutyl ketone and isopropyl alcohol for 30 s, rinsed extensively with isopropyl alcohol, and dried in a stream of nitrogen. The resulting pattern in the photoresist structures was transferred to a chemical surface pattern by using a brief oxygen plasma etch that incorporates highly polar, oxygen-containing moieties in areas of the polymer brush that were unprotected by the photoresist structures and leaves areas of the polymer brush protected by the photoresist structures unmodified.[40] The remaining photoresist was then removed via repeated sonication in warm chlorobenzene, yielding a chemically nanopatterned substrate consisting of stripes of polystyrene brushes alternated with stripes of oxygenated polystyrene brushes.

The chemically nanopatterned substrates were spin-coated with PS-*b*-PMMA block copolymer cast at 6000 rpm from 1.0 to 2.3 wt % solutions in toluene to give films between 18 and 60 nm thick and annealed under vacuum at 190 °C for 72 h. (The block copolymer film thicknesses reported in this paper were adjusted and do not include the underlying 4-nm-thick polystyrene brush layer.) Samples were then slowly quenched to room temperature by first cooling to 100 °C at a rate of 1 °C/min, and then slowly cooling to below 60 °C at an uncontrolled rate before removing from vacuum. The resulting domain structures were analyzed in plan-view by using field emission scanning electron microscopy (LEO-1550 VP), atomic force microscopy (Thermomicroscopes), and optical microscopy. Contrast in the SEM images arises because the electron beam damages and removes the PMMA domains. The PS domains appear bright and the PMMA domains appear dark in the SEM images.[41]

Information about the average domain spacing of the annealed block copolymer films was gathered from a two-dimensional fast Fourier transform (2D-FFT) analysis of scanning electron micrographs of the domains in the annealed films. 2D-FFTs of images that were 512 pixels by 512 pixels were interpolated to a 1023 by 1023 pixel grid. The intensities of the FFT power spectra were averaged azimuthally by using 512 rings around the 1023 by 1023 grid, yielding the average azimuthal intensity of the FFT in q-space ($q = 2\pi/L$).

Results and Discussion

A schematic of the experimental procedure used to direct the assembly of cylindrical domains of PS-*b*-PMMA is shown in Figure 1A. A thin layer of polystyrene was grafted to a silicon wafer and coated with a photoresist. The photoresist was patterned with lines and spaces at pattern periods, L_S, ranging from 40 to 50 nm in increments of 2.5 nm. The width of the photoresist lines, W, depends on the exposure dose. The topographic photoresist pattern was transferred to a chemical surface pattern in the grafted polystyrene brush by using an oxygen plasma etch. The chemically nanopatterned substrate was coated with a thin layer of PS-*b*-PMMA block copolymer that forms cylinders in the bulk. The PS block preferentially wets the polystyrene brush, and the PMMA block preferentially wets the polystyrene brush that was chemically modified by the oxygen plasma. A schematic that defines the lattice spacings of the block copolymer and the notation used in this study is shown in Figure 1B. The intercylinder repeat period, L_O, is 44.8 nm for this block copolymer, and the repeat spacing for a row of cylinders, L, is 38.9 nm. The block-copolymer-coated samples were then annealed at 190 °C for 72 h under vacuum to direct the assembly of the cylindrical block copolymer domains. The resulting domain structures were analyzed in plan-view using SEM, AFM, and optical microscopy.

Figure 2 presents SEM images that capture the behavior of cylinder-forming PS-*b*-PMMA films that are initially 19 nm (L/2) thick. (In all micrographs presented in this study, the chemically patterned stripes run from left to right in the micrographs.) At all pattern periods, the asymmetric block copolymer self-assembled into a highly ordered near-substrate layer that aligned with the same periodicity as the lithographically defined chemical surface pattern, as shown in the azimuthally averaged power spectra of the 2D-FFTs shown in Figure 2f. The q-value corresponding to the maximum intensity in these spectra shifted to match the q-value corresponding to the substrate pattern period for all values of L_S. The wetting layers were defect free except over the $L_S = 50$ nm chemical surface pattern, which intermittently exhibited cylindrical domains that were perpendicular to the free surface between two of the lithographically defined lines. The micrographs shown in Figure 2 are representative of the typical behavior of the assembled block copolymers on chemical surface patterns in which $W/L_S \sim 0.5$.

SEM images presented in Figure 3a−e capture the behavior of cylindrical domains on chemical surface patterns with repeat periods, L_S, from 40 to 50 nm in increments of 2.5 nm ($W/L_S \sim 0.5$), in a film with an initial thickness before annealing of 39 nm. The block copolymer thin film assembled to form a half layer of defect-free cylinders at the free surface, with the same repeat period as the underlying chemical surface pattern, on the chemically nanopatterned substrates that had repeat periods, L_S, from 42.5 to 47.5 nm. On the $L_S = 40$ nm and $L_S = 50$ nm chemical surface patterns, however, defect-free ordering of the cylindrical domains was not observed over large areas. These films exhibited defects consisting of PMMA cylinders that were either perpendicular to the free surface or unaligned with the underlying chemical surface pattern. In those regions of the block copolymer domains that were registered with the underlying $L_S = 40$ nm and $L_S = 50$ nm chemical

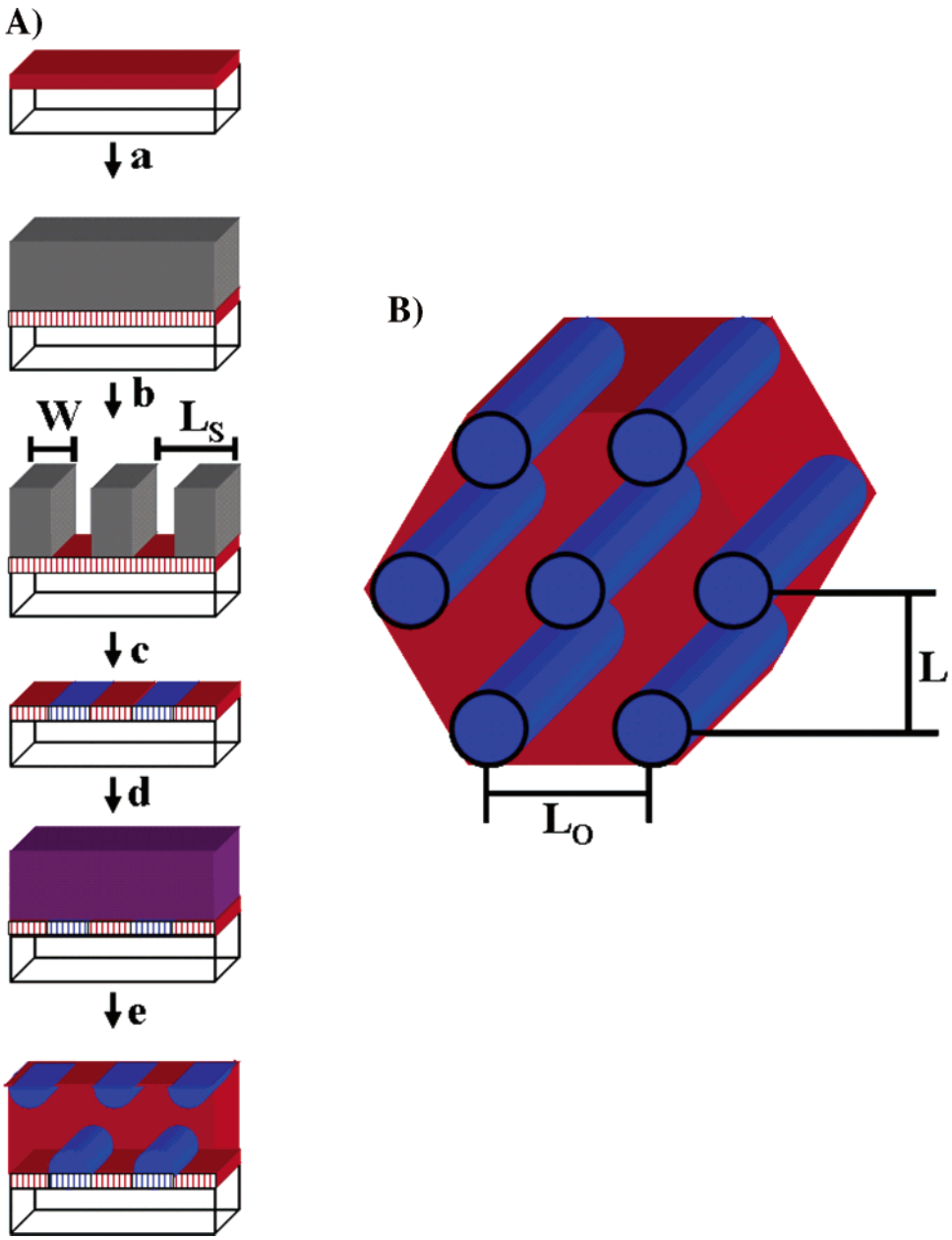

Figure 1. (A) Schematic diagram of the process used to direct the assembly of cylinders parallel to the substrate in registration with the underlying chemical surface pattern (a) a silicon wafer with a polystyrene brush is coated with a photoresist. (b) The photoresist is patterned with lines and spaces using extreme ultraviolet lithography. The widths of the photoresist structures, W, at a given L_S, become more narrow as the exposure time is increased. (c) An oxygen plasma etch generates a chemical surface pattern in the polystyrene brush and the photoresist is removed. (d) The chemically nanopatterned substrates are coated with a thin-block copolymer film and (e) annealed, resulting in surface directed morphologies. (B) Schematic diagram of a cylindrical block copolymer. The intercylinder repeat period is L_O the spacing of rows of cylinders is L.

surface patterns, the domain spacing matched the lithographically defined pattern period. This is captured in the azimuthally averaged power spectra of 2D-FFTs of the images shown in Figure 3f. Over the range 42.5 nm $\leq L_S \leq$ 47.5 nm, the first- and second-order peaks in the azimuthally averaged power spectra are narrow and well-defined, indicating a nearly monodisperse distribution of spacings between cylinders directed by the chemical surface pattern. Contrastingly, the peaks are broad and shift toward the bulk repeat intercylinder spacing of the diblock copolymer domains on chemical surface patterns with periods of $L_S = 40$ nm and $L_S = 50$ nm, indicating that the chemically patterned substrate is no longer directing the assembly of the block copolymer domains over large areas.

Phenomenological Modeling Captures the Effect of $L_S - L_O$ Commensurability. The effect of the chemical surface pattern period/cylinder repeat period commensurability on the ordering of cylinders oriented parallel to the substrate was investigated using a free energy analysis that utilizes a well-known phenomenological model in the literature.[42] The elastic free energy increase per chain for stretching or compressing chains away from L_O in the cylindrical diblock copolymer domains is given by eq 1:

$$\frac{\Delta F_{el}}{kT} = \frac{L_S^2 - L_O^2}{16fN}\left(\frac{\pi^2}{16a^2} - \frac{3}{8a^2}\ln(\varphi_B)\right) \qquad (1)$$

where L_S and L_O are the substrate pattern period and intercylinder repeat period, respectively, N is the degree of polymerization, a is the characteristic length, φ_B is the volume fraction of the minority component, and f is the fraction of minority component monomer units in the chain. For $W/L_S \sim 0.5$, the change in interfacial energy for stretching or compressing the

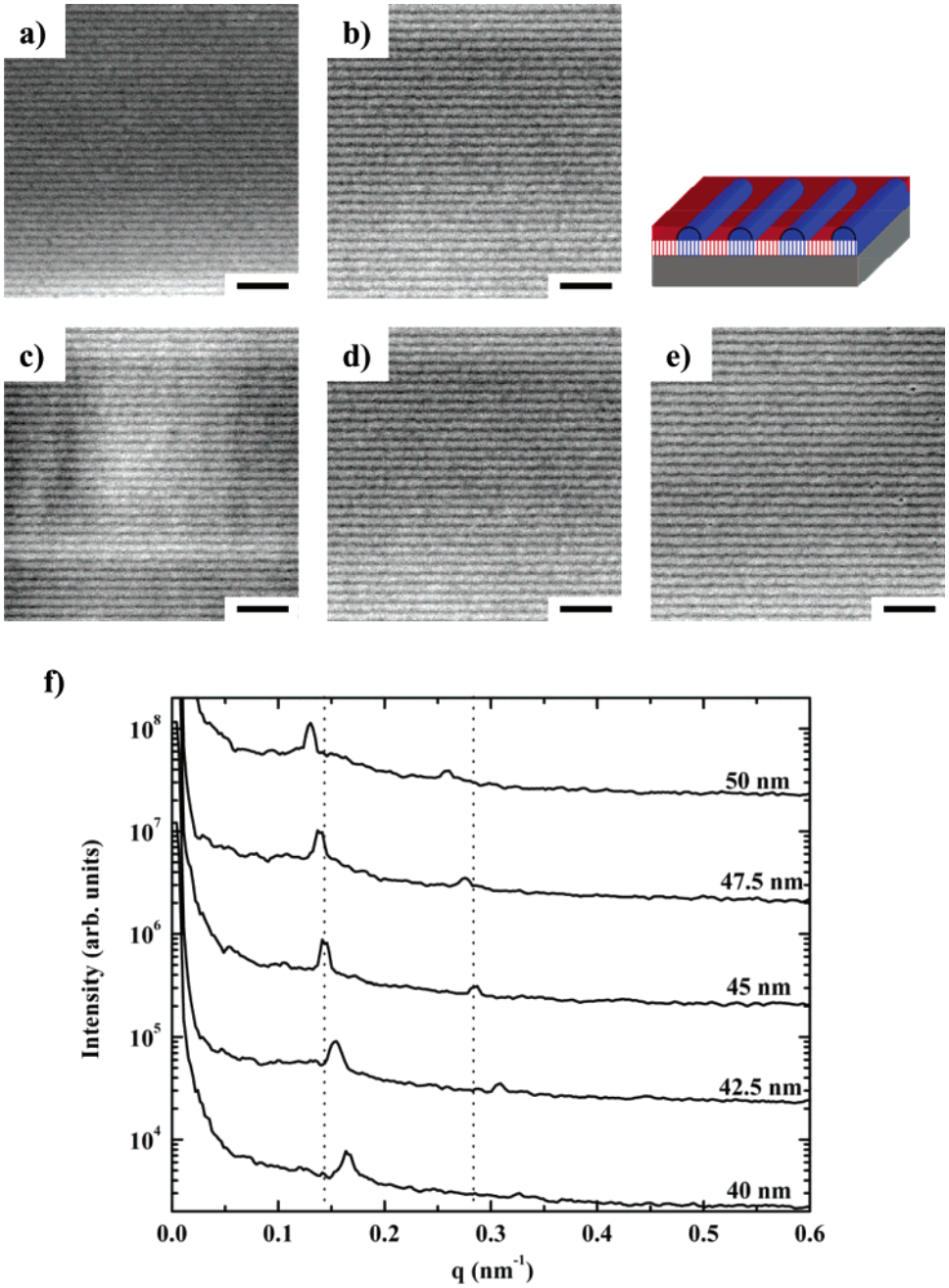

Figure 2. Scanning electron micrographs of self-assembled cylindrical domains in a 19-nm-thick film of PS-*b*-PMMA with $L_O = 44.8$ nm after annealing for 72 h at 190 °C on chemically nanopatterned polystyrene brushes. The periods of the chemically nanopatterned substrates are (a) 40 nm, (b) 42.5 nm, (c) 45 nm, (d) 47.5 nm, and (e) 50 nm. The black scale bars represent 250 nm. (f) Azimuthally averaged 2D-FFT spectra of the images presented in (a−e). The dashed line represents $q_O = 0.140$ nm^{-1} and $2q_O = 0.280$ nm^{-1} for the $L_S = 45$ nm chemical surface pattern. The spectra are offset for clarity. The inset is a schematic of the block copolymer domain behavior.

chains away from L_O is given in eq 2:

$$\frac{\Delta F_{A-B}}{kT} = \left(\frac{1}{L_S} - \frac{1}{L_O}\right) 8fNa\left(\frac{\chi_{A-B}}{6}\right)^{1/2} \quad (2)$$

where χ_{A-B} is the thermodynamic interaction parameter. Finally, reductions in the overall free energy, due to substrate-polymer interactions, over a highest-energy ordered state, assumed to be perfectly assembled cylindrical domains on chemically nanopatterned neutral brushes with a pattern period $L_S = L_O$ and $W/L_S = 0.5$ are given by eq 3.[34]

$$\frac{\Delta F_{interfacial}}{kT} = \frac{\gamma_{PS} - \gamma_{NS}}{2} \frac{M_N}{\rho N_A tkT} \quad (3)$$

Here, M_N is the block copolymer molecular weight, ρ is the polymer density, t is the film thickness, γ_{PS} is the styrene block−styrene brush interfacial energy, and γ_{NS} is the styrene block−neutral brush interfacial energy. Using values of 0.01 erg/cm^2 and 0.15 erg/cm^2 for γ_{PS} and γ_{NS}, respectively,[25] and a film thickness of 18 nm in eq 3, reveals that energy penalties due to stretching and compression of up to 0.064 kT/chain can be allowed in defect-free assembled thin films. Summing the contributions from these two effects in eqs 1 and 2, using published values for a and χ_{AB},[43] reveals that the block copolymer domains can compress or stretch to 39 or 51 nm, respectively, and still give defect-free films. This is in good agreement with our experimental findings. Similar agreement between the model and our experimental results is found when

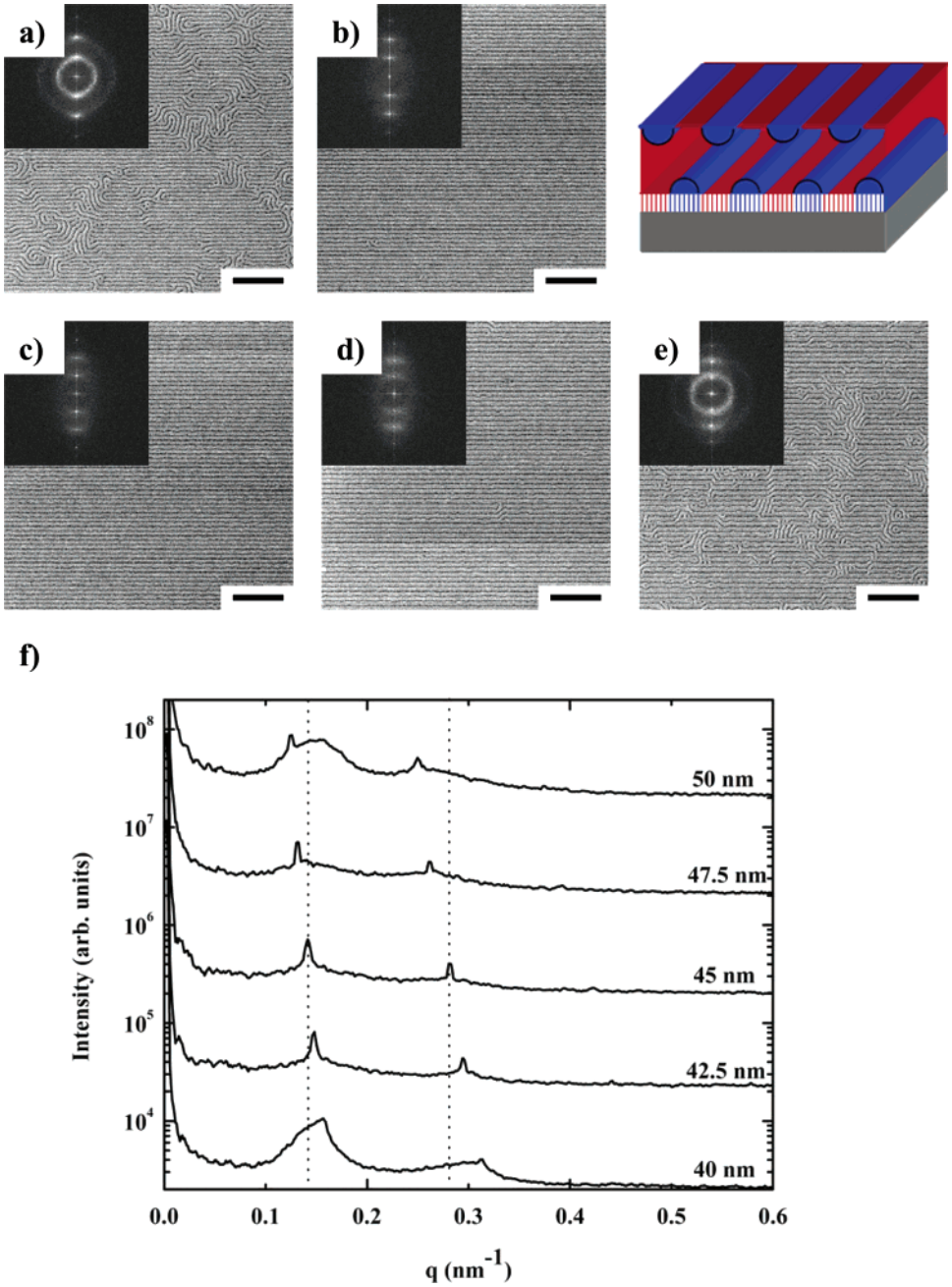

Figure 3. Scanning electron micrographs of self-assembled cylindrical domains in a 39-nm-thick film of PS-*b*-PMMA with $L_O = 44.8$ nm on chemically nanopatterned polystyrene brushes after annealing for 72 h at 190 °C. The periods of the chemically nanopatterned substrates are (a) 40 nm, (b) 42.5 nm, (c) 45 nm, (d) 47.5 nm, and (e) 50 nm. The black scale bars represent 500 nm. (f) Azimuthally averaged 2D-FFT spectra of the images presented in (a−e). The dashed line represents $q_O = 0.140$ nm^{-1} and $2q_O = 0.280$ nm^{-1} for the $L_S = 45$ nm chemical surface pattern. The spectra are offset for clarity. The inset is a schematic of the block copolymer domain behavior.

films with an initial thickness of 39 nm are considered, with the calculations predicting that defect-free films should be observed from 41 to 49 nm, corresponding to stretching and compression penalties of up to 0.031 kT/chain.

Defect-Free Cylinders Only Formed in Films Cast at Thicknesses Commensurate with *L*. Casting films with thicknesses that were commensurate with the thickness of $L/2$ or L was essential for achieving defect-free, directed assembly over large areas. Deviations in the initial film thickness by as little as two nanometers from these thicknesses were enough to induce macroscopic wetting phenomena analogous to the formation of islands and holes on uniform, unpatterned substrates, as shown in Figure 4. In films that were initially cast at a thickness, t, such that $L/2 < t < L$, terraced structures formed on the near-substrate layer, as shown in Figure 4a. In Figure 4a, the topographically higher, terraced structure appears brighter in the scanning electron micrograph, and the topographically lower regions appear darker. These terraced structures were typically 20 nm thick ($\sim L/2$) (as confirmed by AFM), 1 μm wide, and approximately 15−20 μm long and contained a mixture of cylindrical domains that were parallel and perpendicular to the free surface. As the film thickness was increased such that $t \approx L$, a complete half layer of cylinders formed on the near-surface layer. As the initial film thickness was further increased such that $L < t < 3L/2$, a mixture of well-ordered parallel cylinders and terraces containing cylindrical domains that were perpendicular to the free surface formed, as shown in Figure 4b. Again, in Figure 4b, the topographically higher, terraced structure appears brighter in the scanning electron micrograph, and the topographically lower regions appear

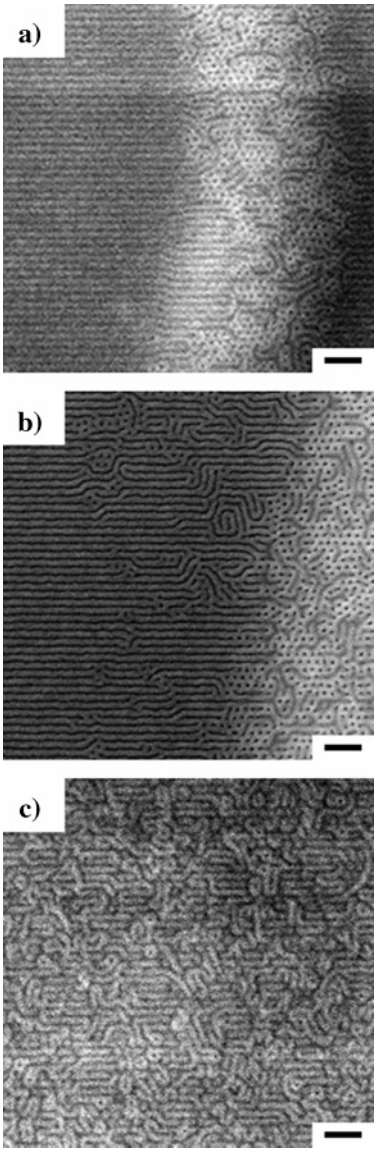

Figure 4. Scanning electron micrographs of self-assembled cylindrical domains of PS-*b*-PMMA with $L_O = 44.8$ nm cast in varying thicknesses on $L_S = 42.5$ nm chemically nanopatterned polystyrene brushes after annealing for 72 h at 190 ° C. Initial film thicknesses are (a) 35 nm, (b) 44 nm, and (c) 57 nm. The black scale bars represent 200 nm.

darker. At an initial, quantized film thickness of $t = 3L/2$, cylinders formed that were oriented parallel to the substrate and did not exhibit any macroscopic wetting phenomena. The parallel cylindrical domains were not directed to assemble in registration with the underlying chemical surface pattern, as shown in Figure 4c. This last result contrasts with previous work by Sundrani et al. that indicated that some alignment in parallel, cylinder-forming diblock copolymers could be induced by topographical surface patterns in thin films up to $5L$ thick.[28,29] Moreover, their results also indicated that ordering could be induced in films that were thicker than the underlying topographic surface pattern.

Quantized film thickness effects may play a role of principal importance in determining the ultimate morphology for cylindrical block copolymer domains aligned by either chemical or topographic surface patterns. To form a single layer of defect-free parallel cylindrical domains in our experiments, the film thickness had to be within 2 nm of the preferred quantized film thickness. Films with initial thicknesses outside this window did not form a single layer of well-aligned cylindrical domains. Similarly, Black et al. performed experiments on parallel cylindrical domains aligned by topographic surface patterns and found that variations of only 2 nm in their initial film thickness could cause the ordering of block copolymer domains to change from defect-free to defect-dominated by using identical annealing conditions.[44] Although it is not clear why the second layer of cylinders shown in Figure 4c is not aligned with the underlying chemical surface pattern, it is likely that our experiments did not sample a film thickness that was sufficiently close to the preferred, quantized film thickness necessary to induce long-range order in the second layer of cylindrical domains.

The terraced structures that formed at film thicknesses that were not commensurate with L or $L/2$ were highly anisotropic in shape when compared to island and hole structures that form on uniform films. This is clearly shown in Figure 5a, which is a low-magnification SEM image of the same film presented in Figure 4 a. As in all of the previously presented micrographs, the underlying chemical surface pattern runs from left to right in the image. It is evident that the topographic features in the self-assembled film are highly extended in the direction perpendicular to the underlying chemically patterned lines. This behavior differs from the behavior of an asymmetric PS-*b*-PMMA film on uniform substrates as shown in Figure 5b, which is a low-magnification scanning electron micrograph of holes formed in this same film on the oxygenated polystyrene brush. The holes shown in this image exhibit more typical, rounded structures that do not preferentially extend in any direction.

Time-lapse optical microscopy was used on a 30-nm-thick film of PS-*b*-PMMA on a chemically nanopatterned substrate with a pattern period $L_S = 42.5$ nm to observe how these terraced structures form (data not shown). These experiments revealed that the terraced structures shown in Figure 5 grow by a spinodal decomposition/nucleation-growth mechanism observed for island and hole formation in lamellar-forming diblock copolymers.[45,46] Initially, small holes form in the film that eventually coalesce as the annealing time increases. The holes coalesce almost uniformly in the direction perpendicular to the chemically patterned stripes. At long annealing times, the terraced structures then ripen and narrow. One possible mechanism by which anisotropic, macroscopic structures form may be that the diblock copolymer chains have a faster diffusion rate along the chemically nanopatterned stripes than across the chemical nanopatterned stripes.

Defect-Free Parallel Cylinders Only Formed on Chemically Striped Surfaces that had Adjacent Stripe Widths That Were Nearly Equal. To obtain defect-free arrays of parallel cylinders, it was necessary to control the relative widths of the stripes that were preferentially wet by each block of the diblock copolymer in addition to controlling the thickness of the as-cast films. The extreme ultraviolet lithography technique used to generate the chemical surface patterns results in variations of the widths of the stripes that are preferentially wet by the styrene and the methyl methacrylate blocks of the block copolymer at a given pattern period. At low exposure doses, wider photoresist features are generated, resulting in wider stripes in the chemically nanopatterned substrate that are preferentially wet by the styrene block of the block copolymer than the stripes that are preferentially wet by the methyl methacrylate block of the block copolymer. At high doses, thinner photoresist features are generated, resulting in thinner stripes that are preferentially wet by the styrene block of the block copolymer than the stripes that are preferentially wet by the methyl methacrylate block of the block copolymer.

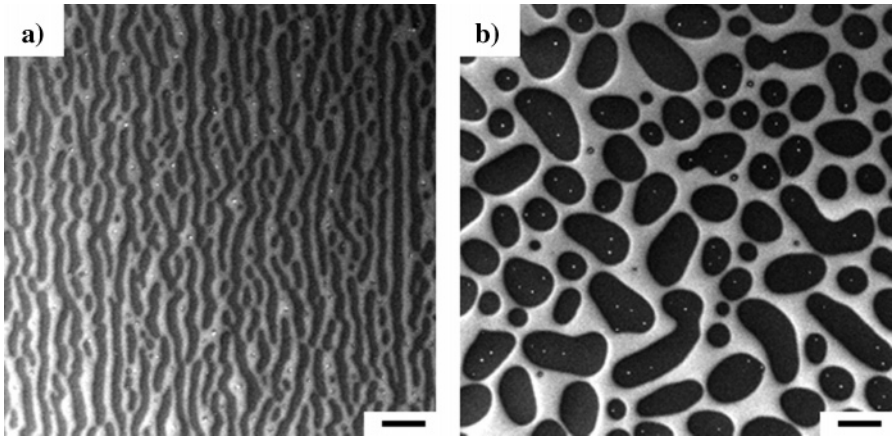

Figure 5. Low-magnification scanning electron micrographs of macroscopic structures formed in a 35-nm-thick film of cylinder-forming PS-*b*-PMMA with $L_O = 44.8$ nm after annealing for 72 h at 190 °C on (a) $L_S = 42.5$ nm chemically nanopatterned polystyrene brushes and (b) an oxygen plasma etched polystyrene brush. The black scale bars represent 50 μm.

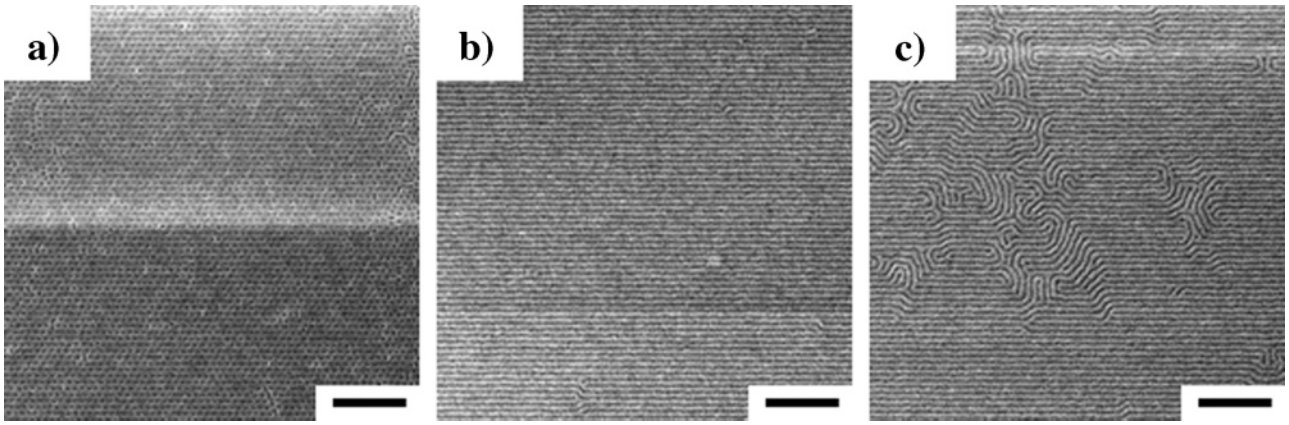

Figure 6. Scanning electron micrographs of self-assembled cylindrical domains in a 38-nm-thick film of PS-*b*-PMMA with $L_O = 44.8$ nm after annealing for 72 h at 190 °C on chemically nanopatterned polystyrene brushes with $L_S = 42.5$ nm. (a) $W/L_S > 0.5$, (b) $W/L_S \approx 0.5$, and (c) $W/L_S < 0.5$. The black scale bars represent 500 nm.

The effect of the relative widths of the stripes that were wet by the two blocks of the block copolymer on the ordering and orientation of the cylindrical domains is shown in a series of SEM images presented in Figure 6. These SEM images capture the domain behavior of a 38-nm-thick PS-*b*-PMMA film on a $L_S = 42.5$ nm chemically nanopatterned substrate with $W/L_S > 0.5$, $W/L_S \approx 0.5$, and $W/L_S < 0.5$ (here W is the width of the stripe that is preferentially wet by the styrene block of the block copolymer). On chemical surface patterns that had wider stripes that were preferentially wet by the styrene block of the block copolymer than the stripes that were preferentially wet by the methyl methacrylate block of the block copolymer, $W/L_S > 0.5$, diblock copolymer domains that appeared in plan-view as cylinders that were oriented perpendicular to the free surface with a high degree of hexagonal ordering formed on the chemically nanopatterned stripes. On chemical surface patterns consisting of adjacent stripes that had nearly equal widths, $W/L_S \approx 0.5$, the cylinders were oriented parallel to the substrate, in registration with the underlying chemical surface pattern. As the width of the regions of the chemically patterned substrate that were preferentially wet by the methyl methacrylate domains of the block copolymer became wider than the regions that were preferentially wet by the styrene domains of the block copolymer, $W/L_S < 0.5$, defects consisting primarily of unregistered cylindrical domains began to appear in the self-assembled domain arrays.

Diblock copolymer domains that appeared in plan-view to be cylinders that were perpendicular to the free surface with a high degree of hexagonal ordering formed on chemical surface patterns with $W/L_S > 0.5$ if the chemical surface pattern period was near commensurate with L. Figure 7 shows SEM images and 2D-FFTs of the cylindrical domains of the block copolymer on chemical surface patterns with $W/L_S > 0.5$ at pattern periods ranging from 40 to 50 nm. On the $L_S = 40$ nm and $L_S = 42.5$ nm, chemical surface patterns that appear in plan-view as PMMA cylinders oriented perpendicular to the free surface formed and displayed a high degree of hexagonal ordering. The $L_S = 45$ nm chemical surface patterns only formed randomly ordered block copolymer domains that appeared in plan-view as cylinders that were oriented perpendicular to the free surface. As the substrate pattern period was further increased to $L_S = 47.5$ nm and $L_S = 50$ nm, the PMMA domains started to form parallel to the substrate, and there was no long-range ordering observed in the domains that were perpendicular to the free surface in plan-view. Azimuthally averaged power spectra of these scanning electron micrographs are presented in Figure 7f. On chemical surface patterns with periods of $L_S = 40$ nm and $L_S = 42.5$ nm, the hexagonal ordering in the cylinders that appeared in plan-view to be perpendicular to the free surface was strong enough to exhibit peaks in these spectra at values of $\sqrt{1}$, $\sqrt{3}$, $\sqrt{4}$, and $\sqrt{7}$ of the highest-intensity first-order Bragg peak. For the cylinders that formed perpendicular to the free surface, on chemical surface patterns with 45 nm $\leq L_S \leq$ 50 nm, only the $\sqrt{1}$ and $\sqrt{4}$ peaks corresponding to randomly ordered cylinders appeared; the $\sqrt{3}$ and $\sqrt{7}$ peaks that would indicate a well-ordered, hexagonally close-packed morphology

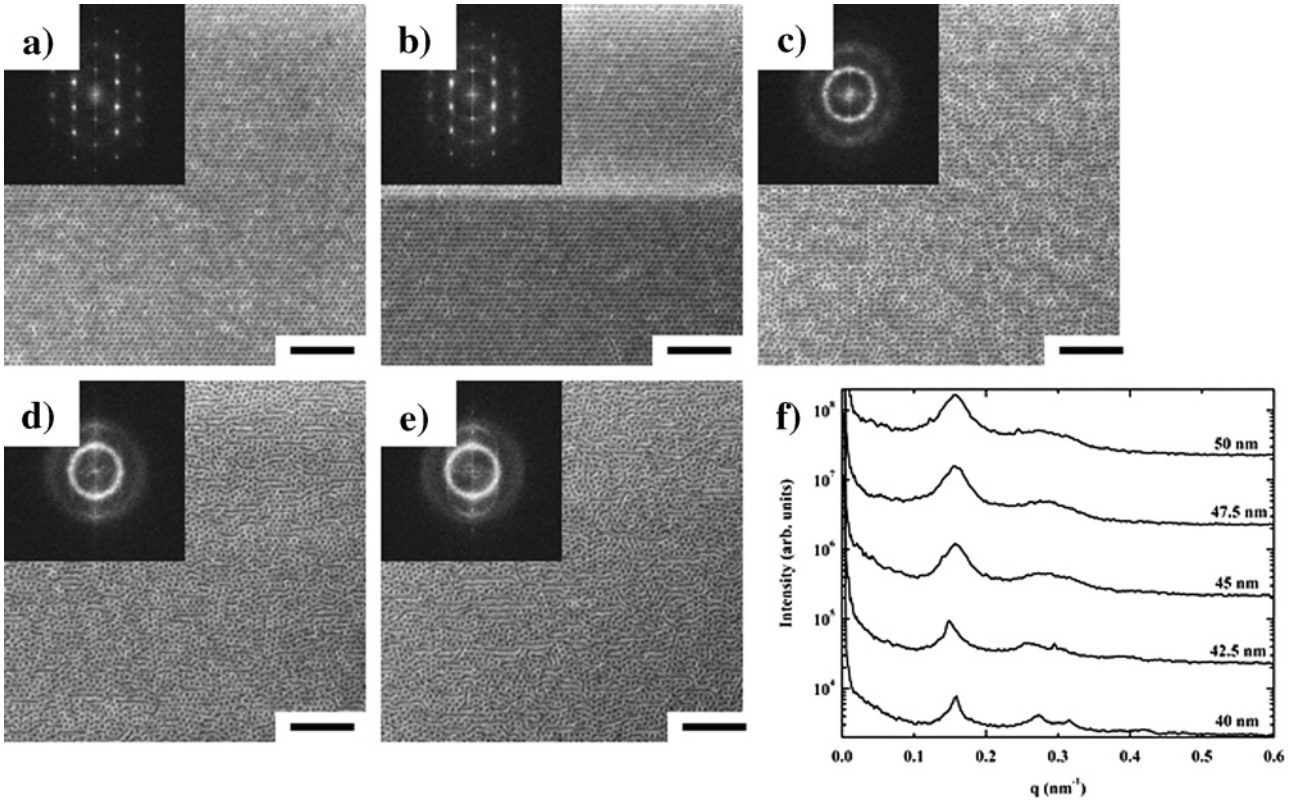

Figure 7. Scanning electron micrographs of self-assembled cylindrical domains oriented perpendicular to the free surface in a 38-nm-thick film of PS-*b*-PMMA with $L_O = 44.8$ nm after annealing for 72 h at 190 °C on chemically nanopatterned polystyrene brushes with pattern periods equal to (a) 40 nm, (b) 42.5 nm, (c) 45 nm, (d) 47.5 nm, and (e) 50 nm. The black scale bars represent 500 nm. (f) Azimuthally averaged 2D-FFT spectra of the images presented in (a−e). The spectra are offset for clarity.

were not observed. Additionally, lower-intensity peaks corresponding to a slight preference for the parallel cylindrical domains to align on the chemical surface patterns also appeared in these spectra.

Although the domains shown in Figure 7 appear to be cylinders oriented perpendicular to the substrate, it is more likely that the morphology of the film consists of necked domains that do not propagate through the entire film. Insight into the formation of such a morphology can be gained from Monte Carlo simulations performed by Wang et al. that looked at the wetting behavior of asymmetric, cylinder-forming diblock copolymers on a variety of chemically nanopatterned substrates.[47,48] Those studies indicated that necked cylindrical domains could form on chemically patterned striped surfaces that were strongly wet by each of the two blocks of the block copolymer, whereas perpendicular cylinders only formed if the chemically striped surfaces consisted of regions that were wet by the majority block of the block copolymer alternated with regions that were neutral to the two blocks of the block copolymer. Given that the experimental conditions of the present study matched the simulation conditions that resulted in necked cylinders, it is likely that the films shown in Figure 7 are actually necked cylinders that have formed on the chemical surface patterns. The formation of a well-ordered near-surface layer that templates a highly ordered hexagonally close-packed morphology at the free surface is consistent with our previously observed results for the time-dependent behavior of lamellar-forming diblock copolymer domains on chemically striped surfaces[49] and the equilibrium behavior of lamellar-forming diblock copolymer domains on chemical surface patterns consisting of square arrays of spots.[50] By using experiments and simulations, these studies found that necked domains with a high degree of hexagonal ordering formed at the free surface, as either kinetic artifacts or equilibrium structures, if lamellae-forming diblock copolymers were annealed on a chemical surface with patterns consisting of stripes or square arrays of spots, respectively. These necked domains did not exhibit registration with the underlying substrate. Moreover, in the case of lamellae-forming diblock copolymers annealed on chemical surface patterns consisting of square arrays of spots, the diblock copolymer formed a bicontinuous morphology that connected the necked domains at the free surface with a near-substrate layer of block copolymer domains that were registered with the underlying chemical surface pattern. Thus, the behavior of the cylindrical diblock copolymer domains on chemical patterned striped surface patterns consisting of $W/L_S \neq 0.5$ likely corresponds to the formation of necked cylindrical domains if $W/L_S > 0.5$ and unregistered parallel cylindrical domains if $W/L_S < 0.5$ that result as the block copolymer domains wet the chemical surface pattern with perfect fidelity and reorder throughout the remainder of the film to adhere to conservation of volume constraints.

The directed assembly of cylinder-forming diblock copolymers over chemically nanopatterned substrates resulted in aligned cylindrical domains with an unprecedented degree of perfection. Previously reported techniques for aligning cylinder-forming diblock copolymers parallel to the substrate, such as graphoepitaxy and shear alignment, have resulted in higher defect densities than those observed in this present study. Recent work by Hammond et al., for example, indicated that graphoepitaxy results in arrays of parallel cylinders that are characterized by a nonzero number of defects in self-assembled films that are at thermodynamic equilibrium.[51] Angelescu et al. found that shear alignment resulted in arrays of cylindrical domains that had defect densities of $\sim 10/\mu m^2$, even under optimal

processing conditions.[32] However, the optimal method for aligning cylinder-forming diblock copolymer domains will ultimately depend on the applications for which these materials will be used. Graphoepitaxy and shear alignment require a much lower degree of infrastructure and less expensive processing than directed assembly on chemically nanopatterned substrates and may be useful for a host of applications. Directed assembly of cylinder-forming diblock copolymers on chemically nanopatterned substrates will thus be advantageous in applications for which the highest degree of patterning perfection in the diblock copolymer domains is required. We recently reported an illustration of this concept with the directed assembly of a cylinder-forming poly(styrene-*b*-*tert*-butyl acrylate) diblock copolymer on both chemically and topographically patterned substrates, which was then followed by a thermally induced phase transition to a spherical diblock copolymer.[11] Both chemically and topographically patterned substrates resulted in arrays of aligned, parallel cylinders with a high degree of orientational order. However, only chemically nanopatterned substrates resulted in well-ordered one-dimensional arrays of spherical domains after the thermally induced phase transition, with many defects forming in the arrays of spheres that were formed from cylindrical domains aligned on topographically patterned substrates. This previous work demonstrates that there are some applications for which the highest degree of cylindrical domain ordering, afforded by directed assembly on chemically nanopatterned substrates, will be necessary.

Conclusions

This work demonstrates the ability of directed assembly to create defect-free arrays of cylinders oriented parallel to the substrate over large areas. The technique offers some advantages over previous methods for ordering cylindrical domains of block copolymers, such as topographically patterned substrates, in that it allows the periodicity of the cylindrical domains to be controlled by the lithographically defined substrate pattern period and forms equilibrium structures that are not characterized by defects. Potential uses of this technique rest primarily in nanomanufacturing and hierarchical device fabrication.

Acknowledgment. Exposures were performed on the X-ray interference beamline at the Swiss Light Source, part of the Paul Scherrer Institut in Villigen Switzerland. This research was supported by the Semiconductor Research Corporation (SRC) (2005-OC-985), the National Science Foundation through the Nanoscale Science and Engineering Center (DMR-0425880), and the Camille Dreyfus Teacher-Scholar Award. This work is based in part upon research conducted at the Synchrotron Radiation Center, University of Wisconsin—Madison, which is supported by the NSF under award no. DMR-0084402. M.P.S. acknowledges a fellowship from the Semiconductor Research Corporation.

References and Notes

(1) Bates, F. S.; Fredrickson, G. H. *Annu. Rev. Phys. Chem.* **1990**, *41*, 525−557.
(2) Bates, F. S.; Fredrickson, G. H. *Phys. Today* **1999**, *52*, 32−38.
(3) Park, M.; Harrison, C.; Chaikin, P. M.; Register, R. A.; Adamson, D. H. *Science* **1997**, *276*, 1401−1404.
(4) Black, C. T.; Guarini, K. W.; Milkove, K. R.; Baker, S. M.; Russell, T. P.; Tuominen, M. T. *Appl. Phys. Lett.* **2001**, *79*, 409−411.
(5) Guarini, K. W.; Black, C. T.; Zhang, Y.; Babich, I. V.; Sikorski, E. M.; Gignac, L. M. Low Voltage, Scalable Nanocrystal Flash Memory Fabricated by Templated Self-Assembly. In *Electron Devices Meeting, 2003, IEDM '03 Technical Digest*; IEEE International, New York, 2003; pp 22.2.1−22.2.4.
(6) Black, C. T.; Guarini, K. W.; Zhang, Y.; Kim, H. J.; Benedict, J.; Sikorski, E.; Babich, I. V.; Milkove, K. R. *IEEE Electron Device Lett.* **2004**, *25*, 622−624.
(7) Thurn-Albrecht, T.; Schotter, J.; Kastle, C. A.; Emley, N.; Shibauchi, T.; Krusin-Elbaum, L.; Guarini, K.; Black, C. T.; Tuominen, M. T.; Russell, T. P. *Science* **2000**, *290*, 2126−2129.
(8) Xiao, S.; Yang, X.; Edwards, E. W.; La, Y. H.; Nealey, P. F. *Nanotechnology* **2005**, S324−S329.
(9) Shin, K.; Leach, K. A.; Goldbach, J. T.; Kim, D. H.; Jho, J. Y.; Tuominen, M.; Hawker, C. J.; Russell, T. P. *Nano Lett.* **2002**, *2*, 933−936.
(10) Lopes, W. A.; Jaeger, H. M. *Nature* **2001**, *414*, 735−738.
(11) La, Y. H.; Edwards, E. W.; Park, S. M.; Nealey, P. F. *Nano Lett.* **2005**, *5*, 1379−1384.
(12) Abes, J. I.; Cohen, R. E.; Ross, C. A. *Chem. Mater* **2003**, *15*, 1125−1131.
(13) Boontongkong, Y.; Cohen, R. E.; Rubner, M. F. *Chem. Mater.* **2000**, *12*, 1628−1633.
(14) Darling, S. B.; Yufa, N. A.; Cisse, A. L.; Bader, S. D.; Sibener, S. J. *Adv Mater.* **2005**, *17*, 2446−2450.
(15) Lin, Y.; Boker, A.; He, J.; Sill, K.; Xiang, H.; Abetz, C.; Li, X.; Wang, J.; Emrick, T.; Long, S.; Wang, Q.; Balazs, A.; Russell, T. P. *Nature* **2005**, *434*, 55−59.
(16) Sohn, B. H.; Cohen, R. E. *Acta Polym.* **1996**, *47*, 340−343.
(17) Sohn, B. H.; Cohen, R. E. *Chem. Mater.* **1997**, *9*, 264−269.
(18) Zehner, R. W.; Lopes, W. A.; Morkved, T. L.; Jaeger, H.; Sita, L. R. *Langmuir* **1998**, *14*, 241−244.
(19) Zehner, R. W.; Sita, L. R. *Langmuir* **1999**, *15*, 6139−6141.
(20) Finnefrock, A. C.; Ulrich, R.; DuChesne, A.; Honeker, C. C.; Schumaker, K.; Unger, K. K.; Gruner, S. M.; Wiesner, U. *Angew. Chem., Int. Ed.* **2001**, *113*, 1248−1251.
(21) Pai, R. A.; Humayan, R.; Schulber, M. T.; Sengupta, A.; Sun, J. N.; Watkins, J. J. *Science* **2004**, *303*, 507−510.
(22) Simon, P. F. W.; Ulrich, R.; Spiess, H. W.; Wiesner, U. *Chem. Mater.* **2001**, *13*, 3463−3486.
(23) Templin, M.; Franck, A.; DuChesne, A.; Leist, H.; Zhang, Y. M.; Ulrich, R.; Schadler, V.; Wiesner, U. *Science* **1997**, *278*, 1795−1798.
(24) Mansky, P.; DeRouchey, J.; Russell, T. P.; Mays, J.; Pitsikalis, M.; Morkved, T.; Jaeger, H. *Macromolecules* **1998**, *31*, 4399−4401.
(25) Mansky, P.; Liu, Y.; Huang, E.; Russell, T. P.; Hawker, C. *Science* **1997**, *275*, 1458−1460.
(26) Morkved, T. L.; Lu, M.; Urbas, A. M.; Ehrichs, E. E.; Jaeger, H. M.; Mansky, P.; Russell, T. P. *Science* **1996**, *273*, 931−933.
(27) Li, H. W.; Huck, W. T. S. *Nano Lett.* **2004**, *4*, 1633−1636.
(28) Sundrani, D.; Darling, S. B.; Sibener, S. J. *Langmuir* **2004**, *20*, 5091−5099.
(29) Sundrani, D.; Darling, S. B.; Sibener, S. J. *Nano Lett.* **2004**, *4*, 273−276.
(30) Kim, S. H.; Misner, M. J.; Russell, T. P. *Adv. Mater.* **2004**, *16*, 2119.
(31) Kim, S. H.; Misner, M. J.; Xu, T.; Kimura, M.; Russell, T. P. *Adv. Mater.* **2004**, *16*, 226.
(32) Angelescu, D. E.; Waller, J. H.; Adamson, D. H.; Deshpande, P.; Chou, S. Y.; Register, R. A.; Chaikin, P. M. *Adv. Mater.* **2004**, *16*, 1736.
(33) Kim, S. O.; Solak, H. H.; Stoykovich, M. P.; Ferrier, N. J.; de Pablo, J. J.; Nealey, P. F. *Nature* **2003**, *424*, 411−414.
(34) Edwards, E. W.; Montague, M. F.; Solak, H. H.; Hawker, C. J.; Nealey, P. F. *Adv. Mater.* **2004**, *16*, 1315.
(35) Stoykovich, M. P.; Muller, M.; Kim, S. O.; Solak, H. H.; Edwards, E. W.; de Pablo, J. J.; Nealey, P. F. *Science* **2005**, *308*, 1442−1446.
(36) Hawker, C. J.; Elce, E.; Dao, J. L.; Volksen, W.; Russell, T. P.; Barclay, G. G. *Macromolecules* **1996**, *29*, 2686−2688.
(37) Husseman, M.; Malmstrom, E. E.; McNamara, M.; Mate, M.; Mecerreyes, D.; Benoit, D. G.; Hedrick, J. L.; Mansky, P.; Huang, E.; Russell, T. P.; Hawker, C. J. *Macromolecules* **1999**, *32*, 1424−1431.
(38) von Werne, T. A.; Germack, D. S.; Hagberg, E. C.; Sheares, V. V.; Hawker, C. J.; Carter, K. R. *J. Am. Chem. Soc.* **2003**, *125*, 3831−3838.
(39) Solak, H. H.; David, C.; Gobrecht, J.; Golovkina, V.; Cerrina, F.; Kim, S. O.; Nealey, P. F. *Microelectron. Eng.* **2003**, *67−8*, 56−62.
(40) Pellerin, K. M.; Himpsel, F. J.; Edwards, E. W.; Nealey, P. F. Unpublished Results.
(41) Huang, E.; Russell, T. P.; Harrison, C.; Chaikin, P.; Register, R. A.; Hawker, C. J.; Mays, J. *Macromolecules* **1998**, *31*, 7641−7650.
(42) Abetz, V.; Stadler, R.; Leibler, L. *Polym. Bull.* **1996**, *37*, 135−142.
(43) Russell, T. P.; Hjelm, R. P.; Seeger, P. A. *Macromolecules* **1990**, *23*, 890−893.

(44) Black, C. T.; Bezencenet, O. *IEEE Trans. Nanotechnol.* **2004**, *3*, 412−415.
(45) Joly, S.; Raquois, A.; Paris, F.; Hamdoun, B.; Auvray, L.; Ausserre, D.; Gallot, Y. *Phys. Rev. Lett.* **1996**, *77*, 4394−4397.
(46) Heier, J.; Sivaniah, E.; Kramer, E. J. *Macromolecules* **1999**, *32*, 9007−9012.
(47) Wang, Q.; Nealey, P. F.; de Pablo, J. J. *Macromolecules* **2001**, *34*, 3458−3470.
(48) Wang, Q.; Nealey, P. F.; de Pablo, J. J. *Macromolecules* **2003**, *36*, 1731−1740.
(49) Edwards, E. W.; Stoykovich, M. P.; Muller, M.; Solak, H. H.; De Pablo, J. J.; Nealey, P. F. *J. Polym. Sci., Part B: Polym. Phys.* **2005**, *43*, 3444−3459.
(50) Daoulas, K. C.; Muller, M.; Stoykovich, M. P.; Park, S. M.; De Pablo, J. J.; Nealey, P. F.; Solak, H. H. *Phys. Rev. Lett.* **2006**, *96*, 036104.
(51) Hammond, M. R.; Cochran, E.; Fredrickson, G. H.; Kramer, E. J. *Macromolecules* **2005**, *38*, 6575−6585.

MA052335C